Exploiting user grouping and energy harvesting in downlink cellular system

Minh-Sang Van Nguyen[1], Huu Phuc Dang[2], Nhan Duc Nguyen[3]
[1]Faculty of Electronics Technology, Industrial University of Ho Chi Minh City (IUH), Ho Chi Minh City, Vietnam
[2]Department of Electrical-Electronics, School of Engineering and Technology, Tra Vinh University, Tra Vinh , Vietnam
[3]Faculty of Engineering, Van Lang University, Ho Chi Minh City, Vietnam

Article Info	ABSTRACT
	A mobile communication system combining energy harvesting with a cooperative non-orthogonal multiple access (NOMA) system is presented in this research. In the proposed scheme, the relay is assumed to have a limited power source, and it will harvest radio energy from the base station (BS) to serve the near and far users. In this scenario, we consider two possible situations during information transmission in the NOMA application system: perfect successive interference cancellation (SIC) and imperfect successive interference cancellation. The system performance is assessed primarily based on closed-form outage probability expressions. Numerical simulations are conducted to examine the outage probability of the proposed scheme and to verify the derived formulas. The study results have proved that the system performance is still good under the imperfect SIC condition, and several optimal parameters to improve the system performance have been found. Moreover, our research results have shown the superior performance of the proposed model compared with current orthogonal multiple access (OMA) networks.

Corresponding Author:

Nhan Duc Nguyen
Faculty of Engineering, Van Lang University
45 Nguyen Khac Nhu St., Co Giang Ward, Dist. 1, Ho Chi Minh City, Vietnam
Email: nhan.nd@vlu.edu.vn

1. INTRODUCTION

Considered a promising wireless access solution for the fifth generation (5G) era, NOMA has great attentions [1]–[10]. According to the non-orthogonal multiple access (NOMA) principle, the transmission request is not orthogonal at the transmitter and the user's signal is stacked in the power domain. As a result, greater spectrum efficiency is possible. More advances compared with traditional orthogonal multiple access (OMA), NOMA-aided transmitter can send signals to multiple terminals over the same resource block, and effective improvement can be obtained in term of sum rate. At the receiver, NOMA systems use successive interference cancellation (SIC) to decode the users' signal. In term of decoding order, other users are considered noise by systems, which prioritize decoding the user with the best channel state.

NOMA was reviewed in reference [11]–[13], and the authors compared typical multiple access approaches to NOMA. Specifically, NOMA is recommended to apply to 5G communication system. NOMA can improve spectrum efficiency due to non-orthogonal transmission and SIC (SE). The normal energy supply is limited for the users in NOMA-aided systems, for example it is difficult to replace the battery in some places and/or limits the system performance improvement. To overcome this difficulty, energy harvesting (EH) architecture is studied to harvest the energy from the surrounding environments. To provide flexible, sustainable and

stable energy supply, radio frequency (RF) energy harvesting [14] allow users harvested the energy from the radio-frequency signals. For example, simultaneous wireless information and power transfer (SWIPT) has been widely explored in emerging systems [15]–[20]. Reference [18] proposed an optimal wireless power method to improve the outage probability by utilizing the harvested RF energy. The RF energy harvesting strategy used in [19] benefits cognitive radio sensor networks.

The authors in [21] studied the resource optimization problem of NOMA heterogeneous small cell networks with SWIPT. Reference [22] took a two-user model for the downlink network and used an EH based incremental relaying cooperative NOMA (IR-EH-NOMA) technique. They developed analytical formulas for the IR-EH-NOMA network's system throughput. In the delay-limited transmission mode, they evaluated the performance of a standard cooperative relaying NOMA network with EH (CR-EH-NOMA), two real situations are examined such as maximal ratio combining (MRC) and imperfect successive interference cancellation.

In addition, the main contribution and novelty of this paper as shown in: 1) we propose a novel relaying communication model that is based on the NOMA protocol and incorporates EH. Especially, the imperfect SIC problem in NOMA is also considered. 2) the closed-forms of outage probability as function of transmit signal-to-noise ratio (SNR) are calculated. Based on the proposed model, we have found some optimal parameters to enhance the system performance. Next, the outage performance is provided in Monte Carlo simulations to validate our analysis. Our research results have shown that the proposed model can improve the performance of the current OMA networks, as well as it demonstrates the feasibility of NOMA applying in the future networks.

2. SYSTEM MODEL

We consider the relaying system containing the BS with $m, (m = 1, \cdots, M)$ antenas intends to serve the near (U_1) and far user (U_2) in the context of NOMA, shown as Figure 1. The BS communicates directly with U_1 and indirectly with U_2 through relay (R) which is able to harvest energy from the BS. In the first phase of communication, the BS will choose the best antenna to broadcasts the superposition signal $x(t) = \sqrt{b_1}x_1 + \sqrt{b_2}x_2$ to U_1 and R, where $x_i, i = (1,2)$ denotes the information symbol to U_i, and b_i denotes the power allocation factor, provided that $b_1 + b_2 = 1$ and $b_1 < b_2$. After receiving the signal from BS, R will perform decoding and forwarding the signal x_2 to U_2 in next phase with the help of SIC technology. In the NOMA protocol, whether the data transmission is successful or not depends mainly on SIC technology. In the following part, we will analyze two possible cases: perfect SIC and imperfect SIC.
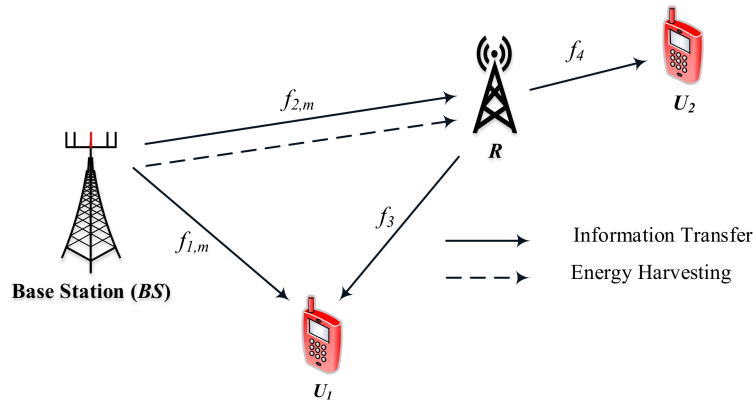

Figure 1. System model

2.1. Scheme 1: perfect successive interference cancellation

In this situation, the received signal regarding link BS-U_1 is given by:

$$y_{SU_1} = \sqrt{P_1}f_{1,m}\left(\sqrt{b_1}x_1 + \sqrt{b_2}x_2\right) + n_{U_1}, \tag{1}$$

where $f_{1,m} \sim CN(0, \eta_1)$ is the channel coefficient between the BS-U_1. n_{U_i} denotes the additive white Gaussian noise (AWGN) at D_i with $n_{U_i} \sim CN(0, N_0)$, P_1 is the power of the BS.

Regarding the link BS-U_1, the received signal-to-interference-plus-noise ratio (SINR) at U_1 to detect U_2's message and its own message, i.e. x_1, are provided by:

$$\gamma_{SU_1}^{(x_2 \to 1)} = \frac{P_1 b_2 |f_{1,m}|^2}{P_1 b_1 |f_{1,m}|^2 + N_0}, \gamma_{SU_1}^{(x_1)} = \frac{P_1 b_1 |f_{1,m}|^2}{N_0}. \tag{2}$$

The R harvests energy from the BS in the first phase and uses this energy to relay the signal to U_1 and U_2 in the next phase. Therefore, by employing power splitting protocol (PS) [20], [21], the signal received at R in the first period is represented as:

$$y_{SR} = (1-\theta) \sqrt{P_1} f_{2,m} \left(\sqrt{b_1} x_1 + \sqrt{b_2} x_2 \right) + n_R, \tag{3}$$

where $f_{2,m} \sim CN(0, \eta_2)$ is the channel coefficient between the BS–R, n_R represents the AWGN at R with $n_R \sim CN(0, N_0)$, θ is the power separation factor.

Also in the first stage, the signal-to-interference-noise ratio (SINR) at R for message detection of U_2 and for its message detection, i.e. x_1, is calculated by:

$$\gamma_{SR}^{(x_2)} = \frac{(1-\theta) P_1 b_2 |f_{2,m}|^2}{(1-\theta) P_1 b_1 |f_{2,m}|^2 + N_0}, \gamma_{SR}^{(x_1)} = \frac{(1-\theta) P_1 b_1 |f_{2,m}|^2}{N_0}. \tag{4}$$

In the second stage of communication, the signal received at U_i, $i = (1, 2)$ is being as:

$$y_{RU_i} = \sqrt{P_2} f_X \left(\sqrt{b_1} x_1 + \sqrt{b_2} x_2 \right) + n_{U_i}, \tag{5}$$

where $X = \{3, 4\}$, P_2 is the power of the R. $f_3 \sim CN(0, \eta_3)$ and $f_4 \sim CN(0, \eta_4)$ are the channel factor of the links R-U_1 and R-U_2. Similarly, the SINR at U_2 to detect its own message, i.e x_2, is provided by:

$$\gamma_{RU_2}^{(x_2)} = \frac{P_2 b_2 |f_4|^2}{P_2 b_1 |f_4|^2 + N_0}. \tag{6}$$

The SINR at U_1 to detect U_2's message and to detect its own message, i.e.x_1, in this stage are calculated by:

$$\gamma_{RU_1}^{(x_2 \to 1)} = \frac{P_2 b_2 |f_3|^2}{P_2 b_1 |f_3|^2 + N_0}, \gamma_{RU_1}^{(x_1)} = \frac{P_2 b_1 |f_3|^2}{N_0}. \tag{7}$$

We assume that U_1 regarding two associated links and hence, the decision rule for selecting one of the links at U_1 in the case of the full selection combining (SC) [22]. Therefore, the instantaneous SINR at user U_1 is written as:

$$\Gamma_{U_1} = \max \left\{ \min \left(\gamma_{SU_1}^{(x_2 \to 1)}, \gamma_{SU_1}^{(x_1)} \right), \min \left(\gamma_{SR}^{(x_1)}, \gamma_{RU_1}^{(x_2 \to 1)}, \gamma_{RU_1}^{(x_1)} \right) \right\}. \tag{8}$$

Moreover, the energy obtained at relay R is provided by $P_2 = \theta \beta P_1 |f_{2,m}|^2$ [19], where β is energy conversion efficiency.

The chosen antenna can be selected to strengthen the BS-U_1, BS-R link as $m^* = \arg \max_{m=1,\cdots,M} \left(|f_{i,m}|^2 \right)$ [23]. Base on [24], the selected channel has CDF, and PDF of $|f_{i,m^*}|^2$, respectively as:

$$F_{|f_{i,m^*}|^2}(x) = 1 - \sum_{m=1}^{M} C_m^M (-1)^{m-1} \exp \left(-\frac{mx}{\eta_i} \right), f_{|f_{i,m^*}|^2}(x)$$
$$= \sum_{m=1}^{M} C_m^M (-1)^{m-1} \frac{m}{\eta_i} \exp \left(-\frac{mx}{\eta_i} \right). \tag{9}$$

2.2. Scheme 2: imperfect successive interference cancellation

In this section, because the imperfections of SIC in real networks are entirely possible, we examine and evaluate the system's performance assuming imperfect SIC at the relay and U_1. Regarding to the imperfect

SIC, the received SINR at BS-U_1 to detect its own message x_1, the received SINR at BS-R to detect its own message x_1 and the received SINR at R-U_1 to detect its own message x_1 are given by:

$$\gamma_{SU_1}^{(ip,x_1)} = \frac{P_1 b_1 |f_{1,m}|^2}{P_1 b_2 \left|\widetilde{f}_{1,m}\right|^2 + N_0}, \gamma_{SR}^{(ip,x_1)} = \frac{(1-\theta) P_1 b_1 |f_{2,m}|^2}{(1-\theta) P_1 b_2 \left|\widetilde{f}_{2,m}\right|^2 + N_0}, \gamma_{RU_1}^{(ip,x_1)} = \frac{P_2 b_1 |f_3|^2}{P_1 b_2 \left|\widetilde{f}_3\right|^2 + N_0}, \quad (10)$$

where $\widetilde{f}_k \sim CN\left(0, \chi_i \eta_i\right), (k = 1, m; 2, m; 3), \chi_i \left(0 \le \chi_i \le 1\right)$ denote the level of residual interference at BS-U_1, BS-R, R-U_1 because of SIC imperfection. As a particular case, $\chi_i = 0$ and $\chi_i = 1$ represent perfect SIC and no SIC, respectively.

3. OUTAGE PROBABILITY
3.1. Sheme 1: perfect successive interference cancellation
3.1.1. Outage probability of U_1
Base on (8), the outage probability (OP) for U_1 can be obtained as [23], [24]:

$$\Phi_1 = \underbrace{\Pr\left\{\min\left(\gamma_{SU_1}^{(x_2 \to 1)}, \gamma_{SU_1}^{(x_1)}\right) < \psi_1\right\}}_{\Theta_1} \underbrace{\Pr\left\{\min\left(\gamma_{SR}^{(x_1)}, \gamma_{RU_1}^{(x_2 \to 1)}, \gamma_{RU_1}^{(x_1)}\right) < \psi_1\right\}}_{\Theta_2}, \quad (11)$$

where $\psi_i = 2^{2R_i} - 1, i = (1,2)$, R_i is target rates of U_i.
Base on (11), Θ_1 can be written as:

$$\Theta_1 = 1 - \Pr\left(|f_{1,m^*}|^2 \ge \Omega\right) = 1 - \sum_{m=1}^{M} C_m^M (-1)^{m-1} \exp\left(-\frac{m\Omega}{\eta_1}\right), \quad (12)$$

where $\Omega = \max\left(\frac{N_0 \psi_1}{P_1(b_2 - \psi_1 b_1)}, \frac{N_0 \psi_1}{P_1 b_1}\right)$.
Base on (11), Θ_2 can be expressed as:

$$\begin{aligned}
\Theta_2 &= 1 - \Pr\left(\gamma_{SR}^{(x_1)} \ge \psi_1\right) \Pr\left(\min\left(\gamma_{RU_1}^{(x_2 \to 1)}, \gamma_{RU_1}^{(x_1)}\right) \ge \psi_1\right) \\
&= 1 - \Pr\left(|f_{2,m^*}|^2 \ge \frac{N_0 \psi_1}{(1-\theta) P_1 b_1}\right) \Pr\left(|f_3|^2 \ge \frac{\Omega}{|f_{2,m^*}|^2 \theta \beta}\right) \\
&= \sum_{m=1}^{M} \sum_{r=1}^{M} C_m^M C_r^M (-1)^{r+m-2} \exp\left(-\frac{m N_0 \psi_1}{(1-\theta) P_1 b_1 \eta_2}\right) \frac{r}{\eta_2} \int_0^\infty \exp\left(-\frac{4\Omega}{4x\theta\beta\eta_3} - \frac{rx}{\eta_2}\right) dx \\
&= \sum_{m=1}^{M} \sum_{r=1}^{M} C_m^M C_r^M (-1)^{r+m-2} \exp\left(-\frac{m N_0 \psi_1}{(1-\theta) P_1 b_1 \eta_2}\right) \sqrt{\frac{4r\Omega}{\theta\beta\eta_2\eta_3}} K_1\left(\sqrt{\frac{4r\Omega}{\theta\beta\eta_2\eta_3}}\right),
\end{aligned} \quad (13)$$

where the last expression in (13) is derived from the fact that $\int\limits_0^\infty e^{-\frac{\tau}{4y} - \rho y} dy = \sqrt{\frac{\tau}{\rho}} K_1\left(\sqrt{\tau\rho}\right)$ in [25], (3.352.4).
Finally, from (12) and (13) into (11) the exact OP of U_1 can be written as:

$$\begin{aligned}
\Phi_1 &= \left[1 - \sum_{m=1}^{M} C_m^M (-1)^{m-1} \exp\left(-\frac{m\Omega}{\eta_1}\right)\right] \left[1 - \sum_{m=1}^{M} \sum_{r=1}^{M} C_m^M C_r^M (-1)^{r+m-2}\right. \\
&\quad \left. \times \exp\left(-\frac{m N_0 \psi_1}{(1-\theta) P_1 b_1 \eta_2}\right) \sqrt{\frac{4r\Omega}{\theta\beta\eta_2\eta_3}} K_1\left(\sqrt{\frac{4r\Omega}{\theta\beta\eta_2\eta_3}}\right)\right].
\end{aligned} \quad (14)$$

3.1.2. Outage probability of U_2
In this case, an outage event at $U2$ will occur if $U2$ and R are unable to correctly detect $x2$, according to the NOMA principle. As a result, the OP of U_2 can be written as:

$$\Phi_2 = 1 - \Pr\left\{\gamma_{SR}^{(x_2)} \ge \psi_2\right\} \Pr\left\{\gamma_{RU_2}^{(x_2)} \ge \psi_2\right\}. \quad (15)$$

Similar as (14) after several steps, the exact OP of U_2 can be written as:

$$\begin{aligned}
\Phi_2 &= 1 - \sum_{m=1}^{M} \sum_{r=1}^{M} C_m^M C_r^M (-1)^{r+m-2} \exp\left(-\frac{m\psi_2 N_0}{((1-\theta) b_2 - \psi_2 (1-\theta) b_1) P_1 \eta_2}\right) \\
&\quad \times \sqrt{\frac{4m\psi_2 N_0}{(b_2 - \psi_2 b_1)\theta\beta P_1 \eta_2 \eta_4}} K_1\left(\sqrt{\frac{4m\psi_2 N_0}{(b_2 - \psi_2 b_1)\theta\beta P_1 \eta_2 \eta_4}}\right).
\end{aligned} \quad (16)$$

3.2. Sheme 2: imperfect successive interference cancellation

In our proposed system model, U_1 and R are two devices that will apply SIC technology to decode x_1 signals. Therefore, imperfect SIC will not affect the outage performance at U_2. In other words, the outage performance at U_2 in both perfect and imperfect SIC scheme is the same. For that reason, in this part, we only calculate the OP at U_1 is being as:

$$\Phi_{ip,1} = \underbrace{\Pr\left(\gamma_{SU_1}^{(ip,x_1)} < \psi_1\right)}_{\Lambda_1} \underbrace{\Pr\left(\min\left(\gamma_{SR}^{(ip,x_1)}, \gamma_{RU_1}^{(ip,x_1)}\right) < \psi_1\right)}_{\Lambda_2}. \tag{17}$$

Base on (17), Λ_1 is given by:

$$\begin{aligned}
\Lambda_1 &= 1 - \Pr\left\{|f_{1,m^*}|^2 \geq \frac{\psi_1\left(P_1 b_2 |f_{1,m^*}|^2 + N_0\right)}{P_1 b_1}\right\} \\
&= 1 - \sum_{m=1}^{M}\sum_{r=1}^{M} C_m^M C_r^M (-1)^{r+m-2} \frac{r}{\chi_1 \eta_1} \exp\left(-\frac{m\psi_1 N_0}{P_1 b_1 \eta_1}\right) \int_0^\infty \exp\left(-\left(\frac{m\psi_1 b_2}{b_1 \eta_1} + \frac{r}{\chi_1 \eta_1}\right)x\right)dx \\
&= 1 - \sum_{m=1}^{M}\sum_{r=1}^{M} C_m^M C_r^M (-1)^{r+m-2}(-1)^{r+m-2} \frac{rb_1}{m\psi_1 b_2 \chi_1 + rb_1} \exp\left(-\frac{m\psi_1 N_0}{P_1 b_1 \eta_1}\right).
\end{aligned} \tag{18}$$

Then, Λ_2 can written by $\Lambda_2 = 1 - \underbrace{\Pr\left(\gamma_{SR}^{(ip,x_1)} \geq \psi_1\right)}_{\Lambda_{2a}} \underbrace{\Pr\left(\gamma_{RU_1}^{(ip,x_1)} \geq \psi_1\right)}_{\Lambda_{2b}}$. Then, Λ_{2a} is calculated is being as:

$$\begin{aligned}
\Lambda_{2a} &= \Pr\left\{|f_{2,m^*}|^2 \geq \frac{\psi_1\left((1-\theta)P_1 b_2 |f_{2,m^*}|^2 + N_0\right)}{(1-\theta)P_1 b_1}\right\} \\
&= \sum_{m=1}^{M}\sum_{r=1}^{M} C_m^M C_r^M (-1)^{r+m-2} \frac{r}{\chi_2 \eta_2} \exp\left(-\frac{m\psi_1 N_0}{(1-\theta)P_1 b_1 \eta_2}\right) \int_0^\infty \exp\left(-\left(\frac{m\psi_1 b_2}{b_1 \eta_2} + \frac{r}{\chi_2 \eta_2}\right)x\right)dx \\
&= \sum_{m=1}^{M}\sum_{r=1}^{M} C_m^M C_r^M (-1)^{r+m-2} \frac{rb_1}{m\psi_1 b_2 \chi_2 + rb_1} \exp\left(-\frac{m\psi_1 N_0}{(1-\theta)P_1 b_1 \eta_2}\right).
\end{aligned} \tag{19}$$

We focus on the high SNR approximation of Λ_{2b} which is given by:

$$\Lambda_{2b} \approx \Pr\left(|f_3|^2 \geq \frac{\psi_1 b_2 \left|\widetilde{\widetilde{f_3}}\right|^2}{b_1}\right) \approx \frac{1}{\chi_3 \eta_3}\int_0^\infty \exp\left(-\left(\frac{\psi_1 b_2}{b_1 \eta_3} + \frac{1}{\chi_3 \eta_3}\right)x\right)dx \approx \frac{b_1}{\psi_1 b_2 \chi_3 + b_1}. \tag{20}$$

From (18)-(20) into (17), the exact OP of U_1 for imperfect SIC can be written as:

$$\begin{aligned}
\Phi_{ip,1} &= \left[1 - \sum_{m=1}^{M}\sum_{r=1}^{M} C_m^M C_r^M (-1)^{r+m-2} \frac{rb_1}{m\psi_1 b_2 \chi_1 + rb_1} \exp\left(-\frac{m\psi_1 N_0}{P_1 b_1 \eta_1}\right)\right] \\
&\times \left[1 - \sum_{m=1}^{M}\sum_{r=1}^{M} C_m^M C_r^M (-1)^{r+m-2} \frac{rb_1}{m\psi_1 b_2 \chi_2 + rb_1} \frac{b_1}{\psi_1 b_2 \chi_3 + b_1} \exp\left(-\frac{m\psi_1 N_0}{(1-\theta)P_1 b_1 \eta_2}\right)\right].
\end{aligned} \tag{21}$$

4. NUMERICAL RESULTS

In this part, simulation results are provided by using Monte Carlo simulation method to demonstrate the performance of the proposed cooperative NOMA systems. In particular, the following set of parameters are used: $b_1 = 0.25$, $R_1 = R_2 = 0.7$ (bps/Hz), $\theta = \beta = 0.6$, $\eta_1 = \eta_2 = \eta_3 = \eta_4 = 1$, $\chi = \chi_1 = \chi_2 = \chi_3 = 0.1$, $P_1/N_0 = 10$ (dB), $M = 2$. Some simulation parameters are given in the caption and the legend of the figures.

As the observation, Figure 2 and Figure 3 plot the OP for proposed NOMA scheme under two scenarios of perfect SIC and imperfect SIC. Observing the Figure 2, we may conclude that, despite the faulty SIC, the system performance still performs well. User U_1 has superior outage performance than user U_2 over the whole range of transmit SNR at source. More specifically, the system achieves better performance in perfect SIC case and the system performance will get better as the number of antennas increases. Besides, we also found from Figure 3 that the NOMA technique performed better than the conventional OMA technology. Furthermore, when increasing the power splitting coefficient of energy harvesting protocol ,i.e., θ, the system performance

is also better. This proves that our proposed model can improve the performance of existing mobile communication networks.
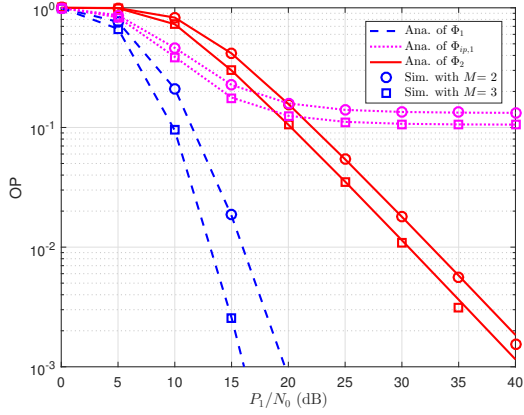

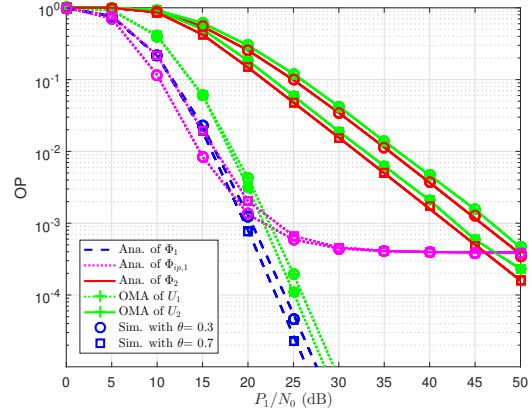Figure 2. Outage performance of U_1 and U_2 versus P_1/N_0 as varying M

Figure 3. Outage performance of U_1, U_2 and OMA versus P_1/N_0 as varying θ

The outage performance is illustrated in Figure 4 as the goal rates are varied. It can be shown that the greater the target rate, the higher the harvested power and the lower the outage performance. Furthermore, when b_1 increases from 0 to 0.35, the perfect SIC mode outperforms the imperfect mode in terms of outage performance. However, according to the principles of NOMA, increasing b_1 means that b_2 is reduced so the performance of U_2 also decreases. Therefore, in order for system performance to be guaranteed for all cases, we obtain the optimal power distribution coefficient at values around $b_1 = 0.2$. We can easily see from Figure 5 that the perfect SIC case always achieves better performance than the imperfect SIC case for different values of SINR and R_1. In addition, it can also be observed that the system performance is significantly enhanced at small target rates and high SINR.
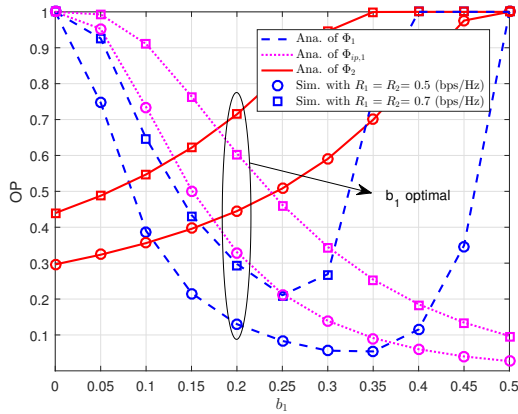

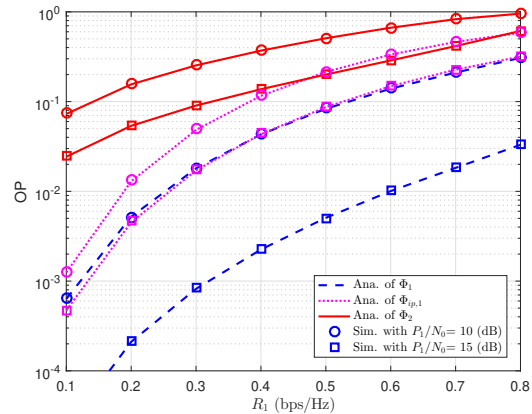Figure 4. Outage performance of U_1, U_2 versus b_1 as varying $R_1 = R_2$

Figure 5. Outage performance of U_1, U_2 versus $R_1 = R_2$ as varying P_1/N_0

5. CONCLUSION

In this work, we investigated the impact of energy harvesting on the system performance metric of the NOMA system. Simultaneously, the issue of NOMA's imperfect SIC was investigated. We focus on outage probability for two users with fixed power allocation factors adopted to make differences among two user. When the relay is able harvest larger amount of harvested energy, the system performance can be improved

significantly. Further, we have obtained optimal values of several important parameters that help to greatly improve the system performance. Finally, having more antennas at the source improves the system's outage performance, and our findings suggest that the proposed model can increase the performance of current OMA networks while also demonstrating the potential of using NOMA in future networks.

ACKNOWLEDGEMENT

REFERENCES

[1] Z. Ding *et al.*, "Application of Non-Orthogonal Multiple Access in LTE and 5G Networks," *IEEE Communications Magazine*, vol. 55, no.2, pp. 185-191, 2017, doi: 10.1109/MCOM.2017.1500657CM.

[2] Z. Ding, X. Lei, G. K. Karagiannidis, R. Schober, J. Yuan, and V. K. Bhargava, "A Survey on Non-Orthogonal Multiple Access for 5G Networks: Research Challenges and Future Trends," *IEEE Journal on Selected Areas in Communications*, vol. 35, no. 10, pp. 2181-2195, June 2017, doi: 10.1109/JSAC.2017.2725519.

[3] F. Fang, H. Zhang, J. Cheng, S. Roy, and V. C. M. Leung, "Joint User Scheduling and Power Allocation Optimization for Energy-Efficient NOMA Systems With Imperfect CSI," *IEEE Journal on Selected Areas in Communications*, vol. 35, no. 12, pp. 2874-2885, Nov. 2017, doi: 10.1109/JSAC.2017.2777672.

[4] F. Zhou, Y. Wu, Y. Liang, Z. Li, Y. Wang, and K. Wong, "State of the Art, Taxonomy, and Open Issues on Cognitive Radio Networks with NOMA," *IEEE Wireless Communications*, vol. 25, no. 2, pp. 100-108, Jan. 2018, doi: 10.1109/MWC.2018.1700113.

[5] X. Li, M. Liu, C. Deng, P. T. Mathiopoulos, Z. Ding, and Y. Liu, "Full-Duplex Cooperative NOMA Relaying Systems With I/Q Imbalance and Imperfect SIC," *IEEE Wireless Communications Letters*, vol. 9, no. 1, pp. 17-20, 2020.

[6] H. M. Al-Obiedollah *et al.*, "Spectral-Energy Efficiency Trade-Off-Based Beamforming Design for MISO Non-Orthogonal Multiple Access Systems," *IEEE Transactions on Wireless Communications*, vol. 19, no. 10, pp. 6593-6606, 2020, doi: 10.1109/TWC.2020.3004292.

[7] J. Zhang, Y. Zhu, S. Ma, X. Li, and K. -K. Wong, "Large System Analysis of Downlink MISO-NOMA System via Regularized Zero-Forcing Precoding With Imperfect CSIT," *IEEE Communications Letters*, vol. 24, no. 11, pp. 2454-2458, 2020, doi: 10.1109/LCOMM.2020.3010422.

[8] A. Rauniyar, P. E. Engelstad, and O. N. Østerbø, "Performance Analysis of RF Energy Harvesting and Information Transmission Based on NOMA With Interfering Signal for IoT Relay Systems," *IEEE Sensors Journal*, vol. 19, no. 17, pp. 7668-7682, May 2019, doi: 10.1109/JSEN.2019.2914796.

[9] Z. Na, J. Lv, F. Jiang, M. Xiong, and N. Zhao, "Joint Subcarrier and Subsymbol Allocation-Based Simultaneous Wireless Information and Power Transfer for Multiuser GFDM in IoT," *IEEE Internet of Things Journal*, vol. 6, no. 4, pp. 5999-6006, August 2018, doi: 10.1109/JIOT.2018.2865248.

[10] J. Tang, A. Shojaeifard, D. K. C. So, K. Wong, and N. Zhao, "Energy Efficiency Optimization for CoMP-SWIPT Heterogeneous Networks," *IEEE Transactions on Communications*, vol. 66, no. 12, pp. 6368-6383, December 2018, doi: 10.1109/tcomm.2018.2866852.

[11] H. Hu, Y. Liang, H. Zhang, and B. Soong, "Cognitive Radio With Self-Power Recycling," *IEEE Transactions on Vehicular Technology*, vol. 66, no. 6, pp. 6201-6214, December 2016, doi: 10.1109/TVT.2016.2635150.

[12] A. Celik, A. Alsharoa, and A. E. Kamal, "Hybrid Energy Harvesting-Based Cooperative Spectrum Sensing and Access in Heterogeneous Cognitive Radio Networks," *IEEE Transactions on Cognitive Communications and Networking*, vol. 3, no. 1, pp. 37-48, 2017, doi: 10.1109/TCCN.2017.2653185.

[13] J. Ren, J. Hu, D. Zhang, H. Guo, Y. Zhang, and X. Shen, "RF Energy Harvesting and Transfer in Cognitive Radio Sensor Networks: Opportunities and Challenges," *IEEE Communications Magazine*, vol. 56, no. 1, pp. 104-110, January 2018, doi: 10.1109/MCOM.2018.1700519.

[14] J. Kang, I. Kim, and D. I. Kim, "Wireless Information and Power Transfer: Rate-Energy Tradeoff for Nonlinear Energy Harvesting," *IEEE Transactions on Wireless Communications*, vol. 17, no. 3, pp. 1966-1981, December 2017, doi: 10.1109/TWC.2017.2787569.

[15] B. K. S. Lima, D. B. da Costa, L. Yang, F. R. M. Lima, R. Oliveira, and U. S. Dias, "Adaptive Power Factor Allocation for Cooperative Full-Duplex NOMA Systems with Imperfect SIC and Rate Fairness," *IEEE Transactions on Vehicular Technology*, vol. 69, no. 11, pp. 14061-14066, October 2020, doi: 10.1109/TVT.2020.3029791.

[16] V. Aswathi and A. V. Babu, "Full/Half Duplex Cooperative NOMA Under Imperfect Successive Interference Cancellation and Channel State Estimation Errors," *IEEE Access*, vol. 7, pp. 179961-179984, January 2019, doi: 0.1109/ACCESS.2019.2959001.

[17] L. Luo, Q. Li, and J. Cheng, "Performance Analysis of Overlay Cognitive NOMA Systems With Imperfect Successive Interference Cancellation," *IEEE Transactions on Communications*, vol. 68, no. 8, pp. 4709-4722, May 2020, doi: 10.1109/TCOMM.2020.2992471.

[18] J. M. Kang, I. M. Kim, and C. J. Chun, "Deep Learning-Based MIMO-NOMA With Imperfect SIC Decoding," *IEEE Systems Journal*, vol. 14, no. 3, pp. 3414-3417, September 2019, doi: 10.1109/JSYST.2019.2937463.

[19] H. Zhang, M. Feng, K. Long, G. K. Karagiannidis, V. C. M. Leung, and H. V. Poor, "Energy Efficient Resource Management in SWIPT Enabled Heterogeneous Networks With NOMA," *IEEE Transactions on Wireless Communications*, vol. 19, no. 2, pp. 835-845, November 2019, doi: :10.1109/TWC.2019.2948874.

[20] K. Reshma and A. V. Babu, "Throughput Analysis of Energy Harvesting Enabled Incremental Relaying NOMA System," *IEEE Communications Letters*, vol. 24no. 7, pp. 1419-1423, March 2020, doi: 10.1109/LCOMM.2020.2984524.

[21] A. A. Nasir, X. Zhou, S. Durrani, and R. A. Kennedy, "Relaying Protocols for Wireless Energy Harvesting and Information Processing," *IEEE Transactions on Wireless Communications*, vol. 12, no. 7, pp. 3622-3636, December 2012, doi: 10.1109/TWC.2013.062413.122042.

[22] S. Ramabadran, R. Roy, and M. D. Selvaraj, "Performance Comparison of Selection Combining With Full CSI and Switch-and-Examine Combining With and Without Post-Selection," *IEEE Transactions on Vehicular Technology*, vol. 65, no. 5, pp. 3217-3230, May 2016, doi: 10.1109/TVT.2015.2434836.

[23] N. Nguyen, T. Q. Duong, H. Q. Ngo, Z. Hadzi-Velkov, and L. Shu, "Secure 5G Wireless Communications: A Joint Relay Selection and Wireless Power Transfer Approach," *IEEE Access*, vol. 4, pp. 3349-3359, 2016, doi: 10.1109/access.2016.2582719.

[24] L. Fan, N. Yang, T. Q. Duong, M. Elkashlan, and G. K. Karagiannidis, "Exploiting Direct Links for Physical Layer Security in Multiuser Multirelay Networks," *IEEE Transactions on Wireless Communications*, vol. 15, no. 16, pp. 3856-3867, 2016, doi: 10.1109/TWC.2016.2530068.

[25] I. S. Gradshteyn and I. M. Ryzhik, "Table of Integrals, Series and Products," *Mathematics of Computation*, vol. 20, pp. 616, 1966.

BIOGRAPHIES OF AUTHORS

Minh-Sang Van Nguyen ⓘ � 🆂🅲 🅿 was born in Bentre, Vietnam. He is currently pursuing the master's degree in wireless communications. He has worked with the Industrial University of Ho Chi Minh City, Vietnam. His research interests include electronic design, signal processing in wireless communications networks, non-orthogonal multiple access, and physical layer security. He can be contacted at email: nguyenvanminhsang@iuh.edu.vn

Huu-Phuc Dang ⓘ � 🆂🅲 🅿 received the B.S. degree in electrical electronics engineering from the HCMC University of Technology and Education, Vietnam, in 2004, and the M.Eng. degree in automation control from the Ho Chi Minh City University of Transport, Vietnam, 2012. He is currently pursuing the Ph.D. degree with the Ho Chi Minh City University of Technology and Education, Vietnam. He is also working at Tra Vinh University. His research interest includes signal processing in wireless communications networks and automation control. He can be contacted at email: danghuuphuc@tvu.edu.vn

Nhan Duc Nguyen ⓘ � 🆂🅲 🅿 received M.Eng in electronic materials from International Training Institute for Materials Science (ITIMS), Hanoi University of Technology in 1998 and his PhD degree in electrical and computer systems engineering from Monash University, Australia in 2011. He had joined the Faculty of Telecommunications, Post and Telecommunication Institute of Technology in Vietnam as a lecturer since 1999. He served as the Head of Signals and Systems Department at Post and Telecommunication Institute of Technology from 2014 to 2020. He is currently serving as a senior lecturer of Faculty of Engineering cum a Systems Engineering Director of the Innovation Center, Van Lang University. His research interests focus on optical communications, numerical modeling and analysis, signal processing, and sensor data processing in machine learning. He can be contacted at email: nhan.nd@vlu.edu.vn